Journal of Power Sources 194 (2009) 843–846

Contents lists available at ScienceDirect

Journal of Power Sources

journal homepage: www.elsevier.com/locate/jpowsour

Short communication

Superprotonic $KH(PO_3H)$–SiO_2 composite electrolyte for intermediate temperature fuel cells

Alexander S. Bondarenko, Weihua Zhou, Henny J.M. Bouwmeester*

Inorganic Membranes, Faculty of Science and Technology & MESA+ Institute for Nanotechnology, University of Twente, P.O. Box 217, 7500 AE Enschede, The Netherlands

ARTICLE INFO

Article history:
Received 5 February 2009
Received in revised form 25 May 2009
Accepted 2 June 2009
Available online 11 June 2009

Keywords:
Fuel cells
Electrolyte
Composite
Solid acid
Proton conductor

ABSTRACT

Novel thin film composite electrolyte membranes, prepared by dispersion of nano-sized SiO_2 particles in the solid acid compound $KH(PO_3H)$, can be operated under both oxidizing and reducing conditions. Long-term stable proton conductivity is observed at ~140 °C, i.e., slightly above the superprotonic phase transition temperature of $KH(PO_3H)$, under conditions of relatively low humidification ($pH_2O \approx 0.02$ atm).

1. Introduction

Inorganic solid acids like $CsHSO_4$ exhibiting high proton conductivity have potential for use as electrolyte in fuel cells [1–6]. The higher operating temperatures relative to polymer electrolytes, typically in the range 100–250 °C, contribute to improved electrode kinetics and tolerance of known electrode catalysts to CO. Unlike hydrated sulphonated polymers such as Nafion®, no water molecules are required to facilitate proton transport in the solid acids, eliminating the need for continuous humidification of reactant gases. Haile and co-workers have showed the use of solid acid proton conductors both in H_2/O_2 and direct methanol fuel cells [1,2]. Using supported thin CsH_2PO_4 electrolyte membranes on porous stainless steel gas-diffusion electrodes, peak power densities as high as 415 mW cm^{-2} were obtained [3].

Proton conductivity in the solid acid compounds (*e.g.*, sulphates, selenates and phosphates) arises upon a structural phase transformation at elevated temperature. The transition, often referred to as superprotonic phase transition [1,2], creates dynamical disorder in the H-bonded XO_4 network (where X = S, Se, P), enabling fast transport of protons mediated by rapid reorientations of the XO_4 tetrahedra (Grotthuss mechanism)[1,7]. The proton conductivity at the superprotonic phase transition increases abruptly by 2–3 orders of magnitude and may reach values up to 10^{-3} to 10^{-2} S cm^{-1} [1]. To date, however, implementation of superprotonic solid acids in fuel cells is hindered by a poor chemical and mechanical stability [1,7]. The alkali–metal hydrogen sulphates and selenates decompose in hydrogen containing atmospheres [1,8], whereas their dihydrogen phosphate counterparts need significant levels of humidification, for example, up to a water vapour pressure of 0.30 atm for CsH_2PO_4 [2,9], to keep their superprotonic properties. The best superprotonic solid acids known to date are prepared from costly caesium. These facts prompted us in previous research to explore the proton conducting properties of alkali–metal acid phosphites $MH(PO_3H)$ ($M = Li^+$, Na^+, K^+, Rb^+, Cs^+, NH_4^+), in view of their good stability under hydrogen atmospheres [10]. Identification was made of a superprotonic phase transition in potassium dihydrogen phosphite, $KH(PO_3H)$, at an onset temperature of 132 °C, reaching a proton conductivity of 4.2×10^{-3} Ω^{-1} cm^{-1} (at 140 °C). The compound adopts a monoclinic structure at room temperature, and transforms to cubic in the superprotonic phase. In this study, we assess the operational stability window of $KH(PO_3H)$, and demonstrate its viability in thin film $KH(PO_3H)$–SiO_2 composite membranes for use as electrolyte in solid acid fuel cells.

2. Experimental

Powders of $KH(PO_3H)$ were prepared by slow evaporation of an aqueous solution obtained by mixing of H_3PO_3 (99%, Aldrich) and KOH (99.5%, Merck) in molar ratio 1:1. The powders were dried in an oven at ~105 °C for 20 h, ground in an agate mortar and stored in a desiccator due to hygroscopicity of the pure salt. Powders of $KH(PO_3H)$–SiO_2 composites were prepared by dispersing of SiO_2 powder (fumed silica, Aldrich, particle size 14 nm) in an aqueous

* Corresponding author. Tel.: +31 53 489 4611.
E-mail address: h.j.m.bouwmeester@tnw.utwente.nl (H.J.M. Bouwmeester).

0378-7753/$ – see front matter © 2009 Elsevier B.V. All rights reserved.
doi:10.1016/j.jpowsour.2009.06.001

solution of $KH(PO_3H)$, followed by drying at ~105 °C for 20 h. X-ray diffraction data were obtained using a Philips XRD PW3020 diffractometer (50 kV, 35 mA, Cu $K\alpha_1$) at room temperature, and processed with the Philips X'Pert program for phase identification. Thermal analysis of powders, either pure or mixed with Pt/C catalyst (Pt, 50% on carbon black, Alfa Aesar) was carried out using a TG–DTA system (Setaram SETSYS 16/18) under either flowing nitrogen, hydrogen or air (45 ml min^{-1}).

Polycrystalline discs of 10 mm diameter and 1 mm thickness of pure $KH(PO_3H)$, pure SiO_2 and of composites $KH(PO_3H)$–SiO_2 were obtained by isostatic pressing (4×10^8 Pa). The relative density of the pressed specimens was about 90%. Thin composite $KH(PO_3H)$–SiO_2 films on a Pt-coated silicon wafer were prepared by dip coating from an aqueous suspension at concentration 200 g l^{-1} with ratio $KH(PO_3H):SiO_2$ = 4:1 by weight. The films were dried in an oven at 45 °C for 10 h and then at 100 °C for ~24 h. For conductivity measurements, platinum electrodes were sputtered using a JOEL JFC-1300 auto coating machine (deposition rate 20 nm min^{-1}).

Conductivity measurements were performed using electrochemical impedance spectroscopy (EIS) using a PGstat20 Autolab Potentiostat (ECO-Chemie) with integrated frequency response analyzer. An excitation voltage with amplitude 10 mV was used to ensure that measurements were performed in the linear regime. No bias voltage was applied. Measurements were performed under flowing dry nitrogen or humidified air (45 ml min^{-1}) at atmospheric pressure. Humidification of the air was performed by passing the gas through a water bubbler held at 21 °C. The temperature of measurement was varied stepwise with a heating/cooling rate of 0.8 K min^{-1}. Spectra were recorded over the frequency range 0.5 MHz to 100 Hz below the superprotonic phase transition (T_s), and from 50 kHz to 100 or 10 Hz above T_s. Data analysis was carried out using complex nonlinear least squares fitting routines [11,12]. Impedance data obtained were checked on their validity using a Kramer-Kronig transformation test program [13].

3. Results and discussion

Fig. 1 shows the results of differential thermal analysis (DTA) and thermogravimetry (TG) of $KH(PO_3H)$ under dry nitrogen, in air with $pH_2O \approx 0.02$ atm, and in a dry mixture of hydrogen and nitrogen at pH_2 = 0.05 atm. A series of thermal events accompanied by weight losses are disclosed. The first endothermic peak (Fig. 1b) observed at ~132 °C is associated with the superprotonic phase transition occurring in $KH(PO_3H)$ (Fig. 2a). The superprotonic phase transition is apparent in each of the test atmospheres, and is accompanied by a small weight loss (<1 wt%). A gradual weight loss due to partial dehydration is observed upon further heating. This weight loss is independent of whether the atmosphere is reducing or oxidizing, even when the solid acid is mixed with a Pt catalyst. The weight loss becomes more pronounced after endothermic melting at ~195 °C. The weight loss plateau in dry nitrogen observed at the highest temperature covered by experiment would correspond with the formation of KPO_2 [10]. Note further from Fig. 1a that oxidation of $KH(PO_3H)$ in air starts at a temperature around 250 °C, which is far higher than the melting temperature, and far beyond the temperature range where $KH(PO_3H)$ might be used as electrolyte.

The mechanical properties of solid acids may be improved by uniform dispersion of ultrafine oxide particles. Arrhenius plots of the proton conductivity of $KH(PO_3H)$–SiO_2 composites, containing 0–50 wt% of silica (with a particle size of ~14 nm), are shown in Fig. 2b. The superprotonic conductivity decreases with increasing the mass fraction of silica, due to the reduced volume for proton migration as well as the blocking effect of silica grains. At the lowest temperatures, that is, far below the superprotonic transi-

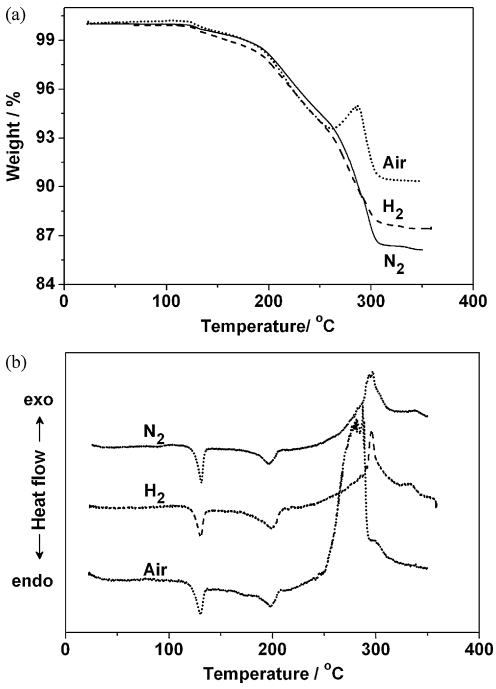

Fig. 1. Thermal analysis of $KH(PO_3H)$ powder under different atmospheres. (a) Thermogravimetry (TG) and (b) differential thermal analysis (DTA) under dry nitrogen, a mixture of N_2 and H_2 (pH_2 = 0.05 atm), and air ($pH_2O \approx 0.02$ atm).

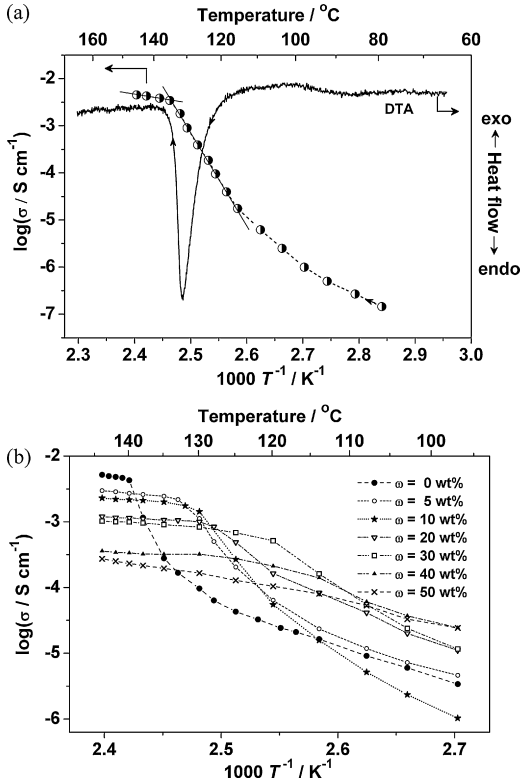

Fig. 2. Dependence of proton conductivity on temperature for (a) pure $KH(PO_3H)$ (first heating scan under dry N_2), and (b) $KH(PO_3H)$–SiO_2 composites (air; $pH_2O \approx 0.02$ atm) at different mass fractions, ω, of SiO_2 (particle size ~14 nm) in the samples. Also shown in (a) are data for pure $KH(PO_3H)$ from differential thermal analysis (DTA) under dry nitrogen. Solid and dashed lines are a guide to the eye.

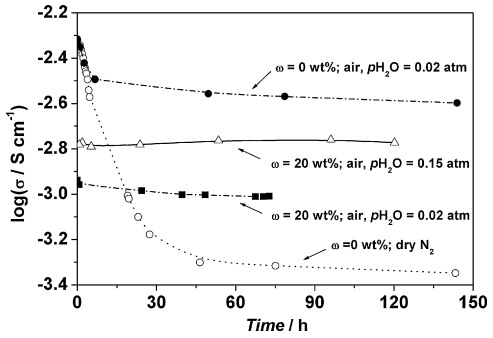

Fig. 3. Time dependence of the superprotonic conductivity of pure $KH(PO_3H)$ and composite $KH(PO_3H)$–SiO_2 at 140 °C in different atmospheres. ω denotes the mass fraction of SiO_2 (particle size ~ 14 nm) in the composites.

tion temperature, however, the conductivity is found to increase with the mass fraction of silica. Similar observations have been made for SiO_2-based composite electrolytes prepared from solid acids $CsHSO_4$ [14–18], CsH_2PO_4 [19], $Cs_3(HSO_4)_2H_2PO_4$ [20] and $CsH_5(PO_4)_2$ [21]. The conductivity of pure silica in humidified air was found not to exceed $\sim 1 \times 10^{-6}\ \Omega^{-1}\ cm^{-1}$. The observed conductivity enhancement at low temperatures is rather interpreted to reflect the formation of highly disordered or space charge regions with enhanced conductivity (due to accumulation of charge carriers) in the close vicinity of the SiO_2 dispersoids. Note from Fig. 2b that the dispersion of SiO_2 also lowers the onset temperature of the superprotonic phase transition. The results show the dispersion affects the thermodynamics of the disordering of the H-bond network. This conclusion is also confirmed by data from thermal analysis, where the endothermic peak temperature associated with the superprotonic transition decreases from ~132 °C as observed for pure $KH(PO_3H)$ to ~115 °C for the composite with 40 wt% of silica (see Supporting Information). The data from thermal analysis also reveal that, in addition to a decrease in transition temperature, the enthalpy of the transition is reduced considerably. For 50 wt% of silica the phase transition is almost suppressed (see Supporting Information). A possible explanation is that the presence of a highly defective region and/or altered distribution of protons at the dispersoid–host interface reduces the number of H-bonds in the ordered hydrogen-bond XO_4 network. Recalling that proton conductivity in the solid acids is characterized by a cooperative rotational disorder of the XO_4 tetrahedra, decreasing the number of H-bonds reduces the enthalpy of the phase transition, and, consequently, the transition temperature.

Fig. 3 shows that the superprotonic conductivity of pure $KH(PO_3H)$ in dry nitrogen gradually decreases with time due to slow dehydration. Dehydration causes samples to lose much of their mechanical strength. A water partial pressure as low as ~0.02 atm, however, turns out to be sufficient to suppress slow dehydration of $KH(PO_3H)$. Both a stable proton conductivity ($\sim 1.15 \times 10^{-3}\ \Omega^{-1}\ cm^{-1}$ at 140 °C) in humidified air (H_2O-saturated, at room temperature) and good mechanical properties are observed for composite electrolytes containing a mass fraction of 20 wt% of silica. Besides the improvement of its mechanical properties, dispersion with fine particles of SiO_2 is found to reduce hygroscopicity of $KH(PO_3H)$.

Reducing the electrolyte thickness is a preferable way to reduce ohmic losses. Fig. 4 shows typical scanning electron micrographs (SEM) of composite $KH(PO_3H)$–SiO_2 electrolyte films produced by dip-coating from a suspension. The high-temperature specific conductivity of the thin films corresponds with that measured for pressed specimens. The area specific resistance (ASR) decreases linearly with film thickness to reach $\sim 1\ \Omega\ cm^2$ at the lowest value within the experimental range of 10–50 μm (see insert in Fig. 4).

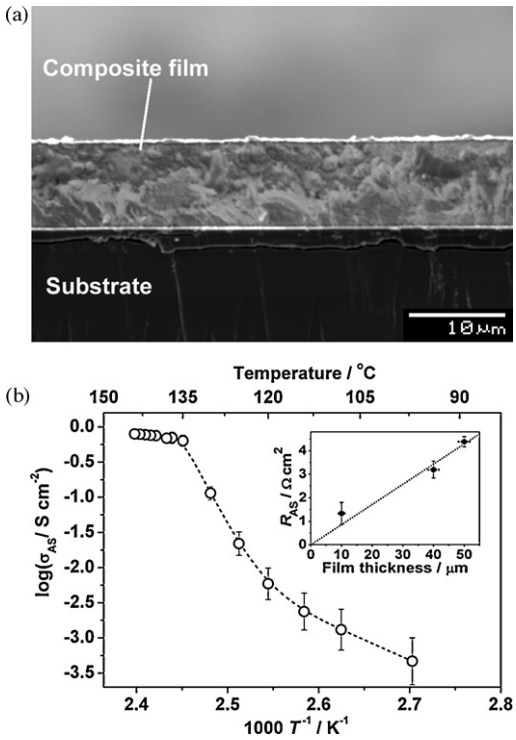

Fig. 4. (a) Cross-sectional scanning electron microscopy (SEM) image of a $KH(PO_3H)$–SiO_2 film ($\omega(SiO_2) = 20$ wt%), and (b) Arrhenius plot of the area specific conductivity (σ_{AS}) of the film with thickness ~10 μm. The insert shows the dependence of the area specific resistance (ASR) on film thickness at 140 °C.

Preliminary fuel cell tests using the $KH(PO_3H)$–SiO_2 electrolyte, commercial Pt/C catalyst, and humidified air and $H_2(5\%)/N_2$ gas mixture showed the open circuit potential of about 0.8 V. It is below the theoretical value of about 1.2 V at this temperature, probably, due to some H_2 leakage through the membrane, and further technological optimisations are required.

In conclusion, the superprotonic conductivity of $KH(PO_3H)$ resembles that of state-of-the-art solid acid electrolytes. Unlike sulphate and selenate solid acid electrolytes, $KH(PO_3H)$ can be operated in both oxidizing and reducing atmospheres. Slight humidification of the gases in liquid water at room temperature, with an equivalent pH_2O of 0.02 atm, is sufficient to prevent impairment of the proton conductivity due to dehydration. Dispersion with nano-sized SiO_2 particles leads to improved mechanical properties. The dispersion-strengthened composite electrolyte can be easily made into a thin film in the μm range by dip-coating from a suspension. Most important, the elevated temperature of operation and low humidification requirement of the thin film solid acid electrolyte membranes will lead to significant system simplifications in comparison with polymer electrolyte fuel cells.

Acknowledgement

This research is supported by the Dutch Technology Foundation STW under Project number 06611.

Appendix A. Supplementary data

Supplementary data associated with this article can be found, in the online version, at doi:10.1016/j.jpowsour.2009.06.001.

References

[1] S.M. Haile, D.A. Boysen, C.R.I. Chisholm, R.B. Merle, Nature 410 (2001) 910–913.

[2] D.A. Boysen, T. Uda, C.R.I. Chisholm, S.M. Haile, Science 303 (2004) 68–70.
[3] T. Uda, S.M. Haile, Electrochem. Solid-State Lett. 8 (2005) A245–A246.
[4] T. Kukino, R. Kikuchia, T. Takeguchi, T. Matsui, K. Eguchi, Solid State Ionics 176 (2005) 1845–1848.
[5] S.M. Haile, C.R.I. Chisholm, K. Sasaki, D.A. Boysen, T. Uda, Faraday Discuss. 134 (2007) 17–39.
[6] D.A. Boysen, C.R.I. Chisholm, S.M. Haile, S.R. Narayananb, J. Electrochem. Soc. 147 (2000) 3610–3613.
[7] A.I. Baranov, V.V. Grebenev, A.N. Khodan, V.V. Dolbinina, E.P. Efremova, Solid State Ionics 176 (2005) 2871–2874.
[8] T. Uda, D.A. Boysen, S.M. Haile, Solid State Ionics 176 (2005) 127–133.
[9] J. Otomo, N. Minagawa, C.-J. Wen, K. Eguchi, H. Takahashi, Solid State Ionics 156 (2003) 357–369.
[10] W. Zhou, A. Bondarenko, B.A. Boukamp, H.J.M. Bouwmeester, Solid State Ionics 179 (2008) 380–384.
[11] B.A. Boukamp, Solid State Ionics 20 (1986) 31–44.
[12] A.S. Bondarenko, G.A. Ragoisha, in: A.L. Pomerantsev (Ed.), Progress in Chemometrics Research, Nova Science Publishers, New York, 2005, pp. 89–102, Chapter 7.
[13] B.A. Boukamp, J. Electrochem. Soc. 142 (1995) 1885–1894.
[14] V.G. Ponomareva, N.V. Uvarov, G.V. Lavrova, E.F. Hairetdinov, Solid State Ionics 90 (1996) 161–166.
[15] V.G. Ponomareva, G.V. Lavrova, L.G. Siminova, Solid State Ionics 118 (1999) 317–323.
[16] V.G. Ponomareva, G.V. Lavrova, Solid State Ionics 145 (2001) 197–204.
[17] H. Shigeoka, J. Otomo, C.-J. Wen, M. Ogura, H. Takahahi, J. Electrochem. Soc. 151 (2004) J76–J83.
[18] S. Wang, J. Otomo, M. Ogura, C.-J. Wen, H. Nagamoto, H. Takahahi, Solid State Ionics 176 (2005) 755–760.
[19] V.G. Ponomareva, E.S. Shutova, Solid State Ionics 178 (2007) 729–734.
[20] V.G. Ponomareva, E.S. Shutova, Solid State Ionics 176 (2005) 2905–2908.
[21] G.V. Lavrova, V.G. Ponomareva, Solid State Ionics 179 (2008) 1170–1173.